Applied Chemical Engineering (2026) Volume 9 Issue 1 ISSN: 2578-2010 (O)
doi: 10.59429/ace.v9i1.5872

ORIGINAL RESEARCH ARTICLE

Spectrophotometric Determination of Iron (III) in Anti-Anemia Drugs and Biological Evaluation of HMNTDABA as an Anticancer Agent

Ayah Kamil Shanbir[1], Shaimaa Mohsen Essa [2*]

[1,2] *Department of Chemistry, College of Education, University of Al-Qadisiyah, Diwaniyah, Iraq*

***Corresponding author:** Shaimaa Mohsen Essa; shaimaa.essa@qu.edu.iq

ABSTRACT

A sensitive and accurate spectrophotometric method was developed for the determination of iron (III) using the azo reagent 2-hydroxy-5-(5-(4-methoxy-3-nitrophenyl)-1,3,4-thiadiazol-2-yl) diazenyl) benzoic acid (HMNTDABA). The reagent was prepared and characterized using UV-Visible spectroscopy, Fourier transform infrared spectroscopy (FT-IR), 1H-NMR spectroscopy, X-ray diffraction (XRD), field emission scanning electron microscopy (FESEM), and elemental analysis (CHNS). The complexation reaction between HMNTDABA and Fe(III) proceeds instantaneously at an optimal wavelength of 485 nm and pH 3.5, yielding a stable yellow complex with a detection limit of 0.104 ppm. The proposed method exhibited excellent precision (S.D. = 0.0012, R.S.D. = 0.17%) and a recovery rate of 97.36%. The stability constant for the 1:2 metal-to-reagent complex was calculated to be 15 × 108 L2.mol−2, with linearity observed across the concentration range of 1–40 ppm. Additionally, the biological activity of HMNTDABA was evaluated against MCF-7 breast cancer cells, revealing concentration-dependent cytotoxic effects and characteristic apoptotic morphological changes. The proposed spectrophotometric method was successfully applied for the quantitative determination of iron(III) in commercial pharmaceutical formulations, including Ferro Strong syrup and Supervit tablets, with results comparable to those obtained by atomic absorption spectroscopy.

Keywords: Thiadiazol, Azo reagent, Biological activity, Spectrophotometric determination of Iron (III)

ARTICLE INFO

Received: 29 December 2025
Accepted: 22 January 2026
Available online: 2 February 2026

Graphical abstract

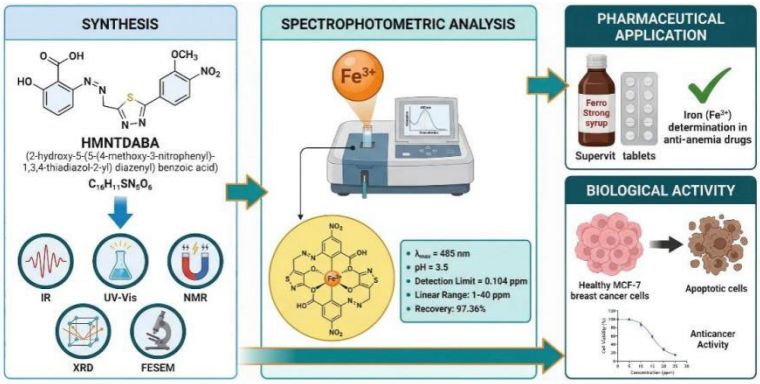

1. Introduction

Organic reagents are regarded as essential materials in analytical chemistry owing to their high efficiency in both qualitative and quantitative detection of metal ions across various sample matrices, including alloys, water, soil, biological tissues, and pharmaceutical formulations [1,2]. These reagents form colored complexes when interacting with metal ions, producing distinct color changes detectable through spectroscopic techniques, particularly UV-Vis absorption

spectroscopy [3,4]. Iron plays a critical role in numerous biological processes, such as oxygen transport, DNA synthesis, and electron transfer [5,6]. Additionally, iron constitutes a fundamental component of modern industrial systems, finding extensive applications in steel production, machinery, and construction materials [7]. Nevertheless, maintaining appropriate iron levels in biological and environmental systems remains crucial, since both deficiency and excess pose significant health and ecological risks [8]. Iron overload conditions, particularly in β-thalassemia major patients, have been associated with developmental complications and ophthalmologic changes [9,10], while nutritional imbalances including obesity have shown significant correlation with children's health status [11,12] In recent years, substantial progress has been made in treating iron-deficiency anemia through effective complexes such as ferric iron tri-maltol (Feraccru or Accrufer) [14]. Furthermore, several analytical techniques have been developed for iron ion determination, including extraction [15], flow injection [16], inductively coupled plasma mass spectrometry (ICP–MS) [17], differential pulse polarography (DPP) [18], and spectrophotometric methods [19], which remain among the most preferred approaches due to their simplicity and sensitivity. Given the significance of organic reagents in spectrophotometric determinations, this study aims to employ the compound 2-hydroxy-5-(5-(4-methoxy-3-nitrophenyl)-1,3,4-thiadiazol-2-yl) diazenyl) benzoic acid (HMNTDABA), synthesized according to the procedure proposed by Hadi, M. K. [20], as an organic reagent. Since the original work did not investigate the iron ion, the reagent was re-prepared in the present research for the spectrophotometric determination of Fe(III). The prepared reagent was characterized using FT–IR and UV–Vis spectroscopy to evaluate its interaction with Fe(III), followed by its application in determining iron levels in pharmaceutical formulations used for anemia treatment. Given that thiadiazole-based azo compounds have demonstrated promising anticancer properties in previous studies, the potential cytotoxic activity of the synthesized reagent HMNTDABA against MCF-7 breast cancer cells was also investigated to explore its dual functionality as both an analytical reagent and a bioactive compound.

2. Materials and methods

2.1. Materials

Fourier transform infrared (FTIR) spectra in the range of 4000–400 cm^{-1} were recorded using a SHIMADZU FTIR-8400S spectrophotometer (Japan), with samples prepared as (KBr) pellets. Ultraviolet–visible (UV–Vis) absorption spectra were obtained using a T80 (UV–Vis) spectrophotometer, while absorbance measurements were carried out on an Apel PD-303 UV–Visible spectrophotometer employing 1 cm quartz cells. Structural characterization of the synthesized reagent was further confirmed by proton nuclear magnetic resonance (^{1}H-NMR) spectroscopy, recorded on a Bruker spectrometer operating at 400 MHz (Switzerland). The surface morphology of the prepared materials was examined using a field emission scanning electron microscope (FE-SEM, MIRA3). Elemental composition, including carbon, hydrogen, nitrogen, and sulfur (CHNS), was determined using a (BBOT) elemental analyzer. Crystallographic features of the synthesized compounds were investigated by X-ray diffraction (XRD) using a D2 Phaser diffractometer, operating over a 2θ angular range of 10–80°. Solution pH values were adjusted and measured using a pH meter, and melting point measurements were carried out employing an (SMP30) Stuart apparatus (UK).

2.2. Chemical and materials

Ethanol Absolute, (99.9%, Germany), Methanol Absolute, (99.8%, Germany), Sodium hydroxide, (97%,Alpha Chemika), Sodium nitrite, (96%, Alpha Chemika), Dimethyl sulphoxide, (98%,J.T.Baker), Acetone, (99.9%, J.T.Baker), Sodium chloride, (98%, CARLO ERBA), Glacial acetic acid, (Analar, Germany), Ferric chloride, (96%, Alpha Chemika), Phosphoryl chloride, (99%, Analar Germany), 4-methoxy-3-nitrobenzoicacid, (98%, Sgma U.S.A), Thiosemicarbazide, (97%, Alpha Chemika), 2-hydroxybenzoic acid, (99%, CARLO ERBA).

2.3. Preparation of HMNTDABA

The Preparation of the azo reagent HMNTDABA was achieved through a two-step procedure adapted and modified from Hadi, M.K. [21], with slight adjustments to optimize yield and purity, the synthetic route is shown in Scheme 1. In the first step, 4-methoxy-3-nitrobenzoic acid (0.6308 g, 0.0032 mol) was reacted with thiosemicarbazide (0.2916 g, 0.0032 mol) in 10 mL of phosphorus oxychloride ($POCl_3$) using a 100 mL round-bottom flask equipped with a magnetic stirrer and reflux condenser. The reaction was maintained under stirring for 3 hours. After cooling to room temperature, 40 mL of distilled water was gradually added with continuous stirring for 4 additional hours. The resulting mixture was filtered, and the filtrate neutralized with 5% KOH solution until reaching pH 7. The product was allowed to settle for 24 hours, then filtered, washed thoroughly with water, dried, and recrystallized from absolute ethanol. In the second stage, 5-(4-methoxy-3-nitrophenyl)-1,3,4-thiadiazol-2-amine (1.0 g, 0.0059 mol) was dissolved in 4 mL of HCl and 30 mL of distilled water, and the solution was cooled to(0–5)°C. A freshly prepared solution of sodium nitrite (0.5 g, 0.0059 mol) in 10 mL of distilled water was added dropwise over 20 minutes to a separately prepared coupling mixture containing 2-hydroxybenzoic acid (0.8214 g, 0.0059 mol) and NaOH (1.0 g, 0.0059 mol) dissolved in 30 mL of chilled water and 5 mL of absolute ethanol. The azo compound began to separate as a brown precipitate. After adjusting the pH to 6, the mixture was left to stand for 24 hours. The solid product was collected by filtration, washed with water, dried, and recrystallized from ethanol to afford the pure HMNTDABA reagent. The yield percentage and physical properties of the final compound were subsequently evaluated [22].

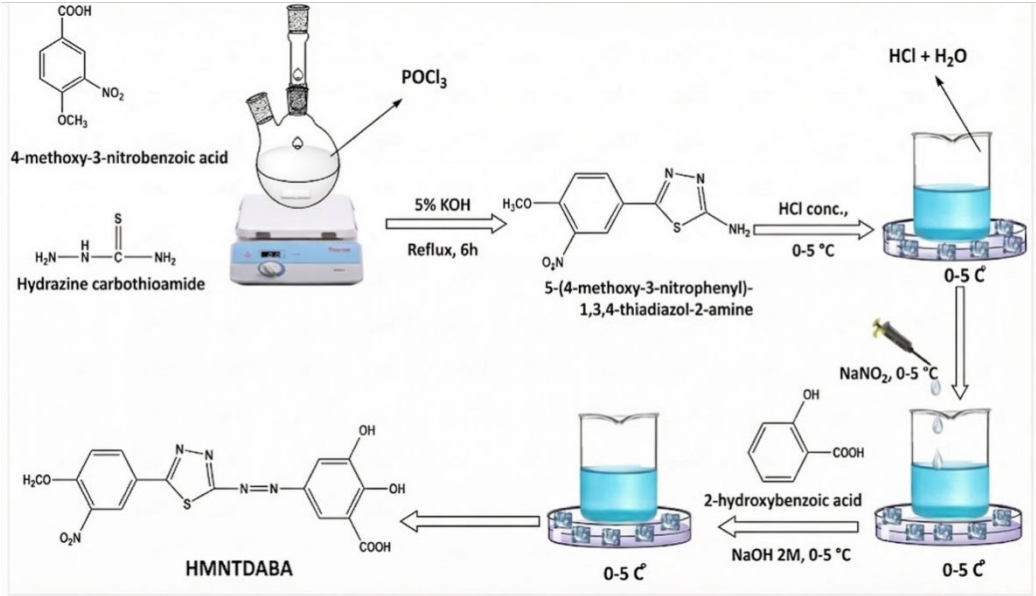

Scheme 1. Method of preparation of the Organic Reagent (HMNTDABA).

2.4. Standard solution

A stock solution of Fe(III) with a concentration of 1000 µg. mL^{-1} was prepared by dissolving (0.3025 g, 0.001865 mol) of ferric chloride ($FeCl_3$) in (1 mL) of concentrated hydrochloric acid, followed by dilution to (100 mL) with distilled water after complete dissolution. Working standard solutions of Fe(III) were obtained by appropriate dilution of the stock solution with distilled water. The standard solution of the organic reagent (HMNTDABA) was prepared at a concentration of (1×10^{-4} M) by dissolving (0.0401 g, 0.00001 mol) of the reagent in (250 mL) of absolute ethanol, with continuous stirring to ensure complete solubility and homogeneity.

3. Results and discussion

3.1. Infrared studies

Analysis of the infrared spectra within the range of (4000-400) cm^{-1} revealed details concerning the coordination mode of the ligands within the complexes, as illustrated in **Figure 1.** These spectra were compared to those of the unbound reagent. The bond in the azo reagent is within the range of (3070.46-3255.62)cm^{-1} refers to the O-H bond of the carboxylic acid and the alcoholic O-H bond, respectively present in the reagent's structure[17], while the range (2947.03-3031.89)cm^{-1} is due to the aromatic C-H bond, and the bond from (1434.94-1550)cm^{-1} corresponds to the N=O and N=N stretching vibrations of the nitro group and the azo group, respectively, in the reagent [23,24], while the bonding is shown at (1660-1620.09)cm^{-1} due to the bonding between C=C and C=O. The FTIR analysis of the iron complex begins with a shift of the apparent peaks compared to the detector, as a prominent band appears at the range (3201.77-3448.66) cm^{-1} indicating the O-H group in the complex formula, while the bonds at (493.77-597.92) cm^{-1} indicate the Fe-N and Fe-O bonds, respectively [25-27].

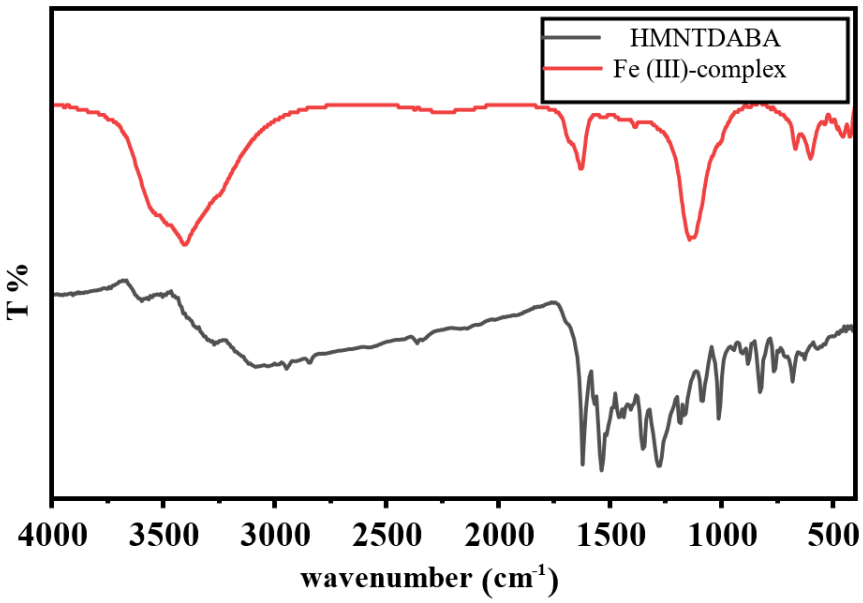

Figure 1. IR spectra of the HMNTDABA and Fe (III) complex.

3.2. Field Emission Scanning Electron Microscope (FESEM)

The FESEM micrographs of the prepared nano reagent, presented in **Figure 2**, illustrate both its morphological and microstructural features. The surface exhibits heterogeneity with numerous irregularities, while the particle sizes remain relatively uniform throughout the sample, indicating a well-controlled synthesis method. Moreover, the observed clustering suggests a tendency for particle aggregation, which may influence the material's overall properties [28].

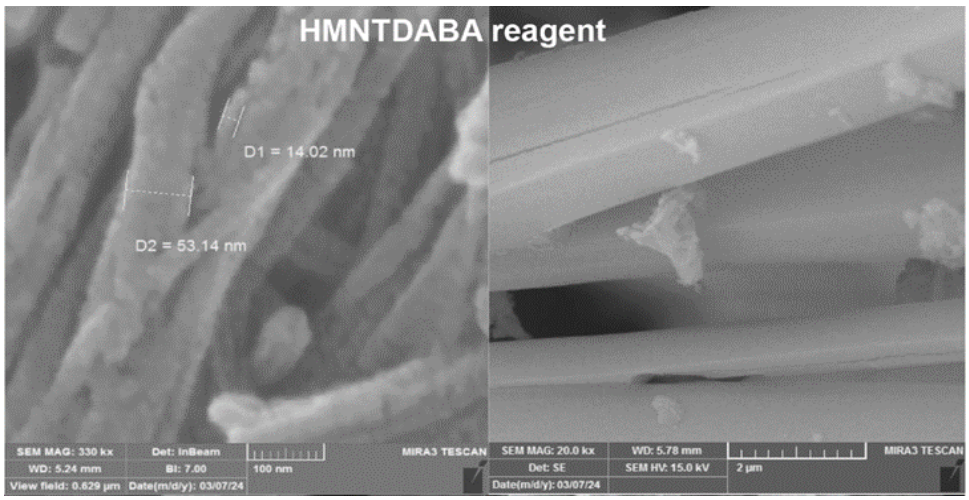

Figure 2. FESEM images of the reagent (HMNTDABA).

3.3. Elemental analysis

Elemental analysis was conducted to identify the elemental composition and quantify the relative percentages of the constituent elements within the prepared compound. As summarized in **Table 1**, the results indicate that the compound primarily consists of carbon (C), hydrogen (H), nitrogen (N), and sulfur (S), with respective mass percentages of 46.999%, 2.723%, 17.139%, and 7.677%. In addition, the experimentally obtained elemental data are in good agreement with the calculated molecular weight of 401.364 g/mol, which corresponds well to the proposed molecular formula $C_{16}H_{11}SN_5O_6$, thereby confirming the structural composition of the compound.

Table 1. C H N S analysis of the compound.

Compound	M.wt	C%		H%		N%		S%	
$C_{16}H_{11}SN_5O_6$	401.364	Found	Calc.	Found	Calc.	Found	Calc.	Found	Calc.
		46.999	47.880	2.723	2.765	17.139	17.449	7.677	7.987

^{1}H-NMR Spectrum

The synthesized compound (HMNTDABA) was characterized using proton nuclear magnetic resonance (^{1}H-NMR) spectroscopy with DMSO-d6 as the solvent, as illustrated in **Figure 3**. The ^{1}H-NMR spectrum exhibited a signal at (2.52 ppm), which is attributed to the solvent residue. An additional signal observed at (3.98 ppm) corresponds to the methyl (O–CH_3) group. Furthermore, two distinct resonances appearing at (6.97 ppm) and (7.45 ppm) are assigned to protons numbered 15 and 18, respectively. The aromatic protons of the compound were identified by a multiplet extending from 7.45 to 8.53 ppm. A signal detected at (4.1 ppm) is ascribed to the hydroxyl (–OH) proton. Moreover, the proton associated with the thiadiazole ring was observed at (8.57 ppm), confirming the successful formation of the proposed molecular structure [29].

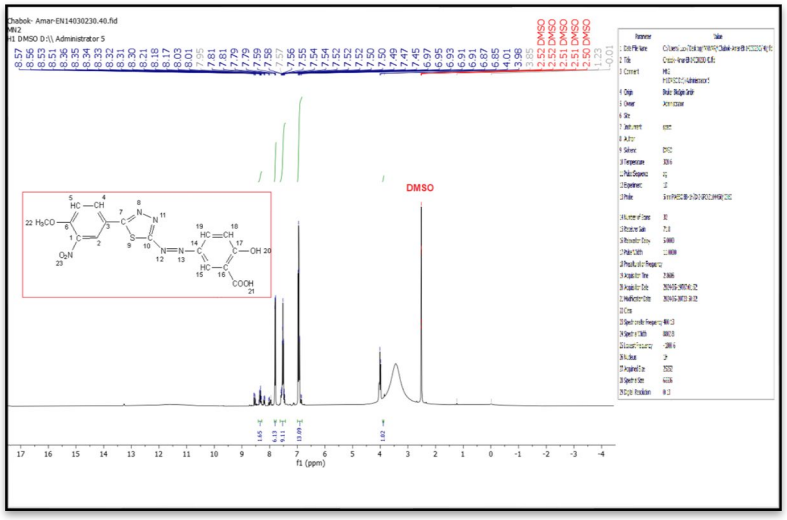

Figure 3. ^{1}H-NMR Spectrum of the organic reagent (HMNTDABA).

3.4. X-Ray diffraction spectrum

The X-ray diffraction XRD analysis of the prepared reagent HMNTDABA is illustrated in **Figure 4**. The obtained diffraction pattern reveals the complex crystalline nature of HMNTDABA, characterized by the presence of several distinct diffraction peaks at different 2θ positions. Notably, prominent peaks are observed at 11.5744°, 31.8404°, and 38.3375°, with the highest intensity recorded at 38.3375°. These reflections indicate the contribution of well-defined structural phases that collectively form the overall diffraction pattern. The XRD results provide valuable insights into the crystallinity and structural characteristics of the newly synthesized reagent [30].

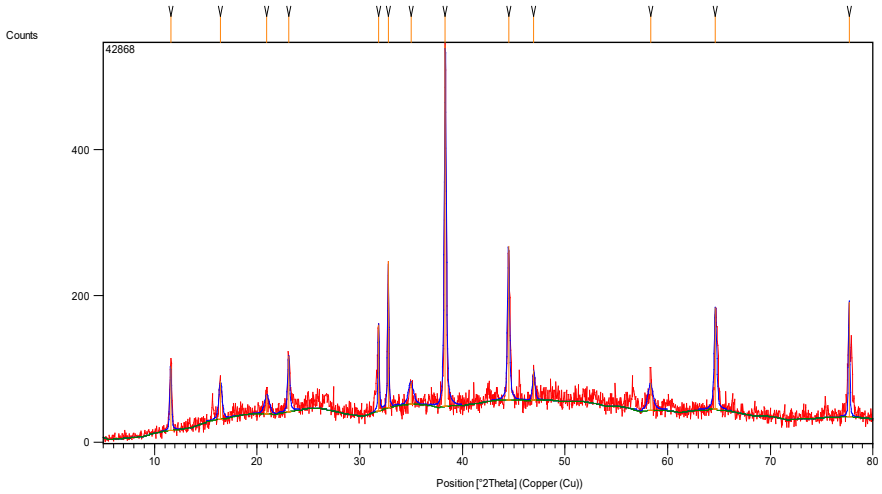

Figure 4. XRD Pattern of the organic reagent (HMNTDABA).

3.5. Absorption spectra and characteristics of the reagent and complex

The UV-Visible absorption spectra of the compounds (HMNTDABA) and the complex Fe(III)-HMNTDABA were recorded. The reagent exhibited a maximum absorbance (λ_{max}) at 297nm, while the iron complex showed its maximum at 485 nm. A yellow complex was formed immediately upon mixing the reagent with Fe(III) in an aqueous solution at pH 3.5. The acidic medium effectively suppressed side reactions that could interfere with complex formation, thereby promoting efficient and stable complexation. This resulted in a distinct bathochromic shift of the absorbance band to 485 nm. The absorbance reached its maximum intensity after 10 minutes and remained stable for at least 24 hours at 50°C temperature, as illustrated in **Figure 5**.

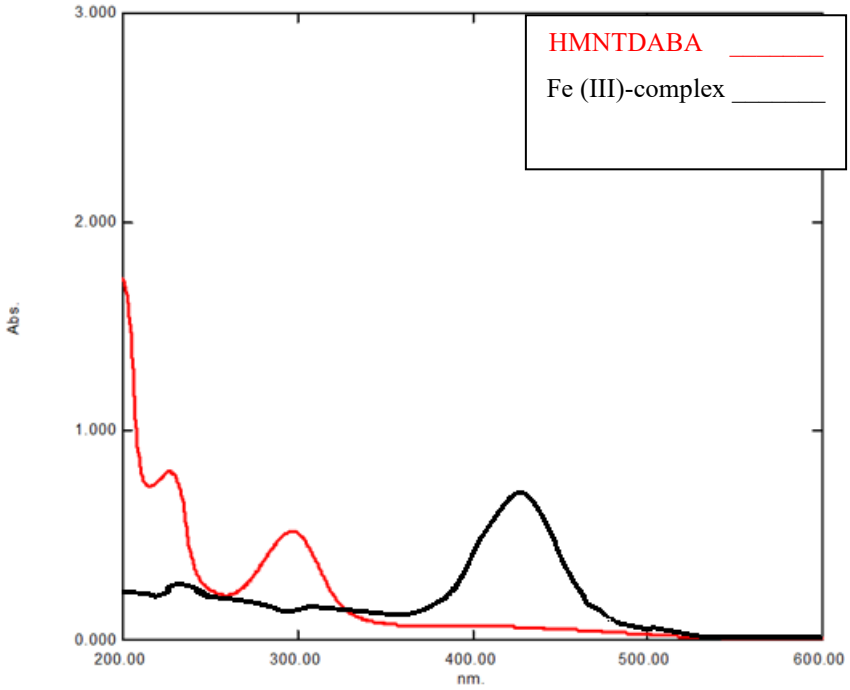

Figure 5. Absorption spectra of Fe(III) ion 20 ppm with the reagent at pH=3.5.

4. Optimum conditions

4.1. Effect of pH on Complex Formed with Fe (III)

The effect of pH on the formation of the Fe(III) complex was investigated by measuring the absorbance at the maximum wavelength (λ_{max}) over a pH range from (2–11) using buffer systems based on the ammonia–acetate pair. A specific concentration of ammonium hydroxide (NH_4OH) was prepared by dissolving an accurately weighed amount in distilled water, followed by mixing measured portions of the ammonia and acetate solutions to obtain the desired buffer. The acetate provides (CH_3COO^-) ions, while ammonia supplies (NH_4^+) ions. The equilibrium between these two systems stabilizes the desired pH values, which were precisely adjusted using a calibrated pH meter to ensure reproducibility during measurement. The results demonstrated that the absorbance reached its maximum at pH = 3.5, which is considered the optimum condition for complex formation. At this pH, the balance between H^+ and OH^- ions minimize secondary reactions that could interfere with or destabilize the Fe(III) complex. Deviation from this value leads to increased ionic interactions, which may affect the stability and composition of the complex. Therefore, pH= 3.5 was identified as the optimal condition for stable Fe(III) complex formation and reliable spectrophotometric determination.

The hydrogen ion concentration plays a crucial role in the formation and stability of complexes. Variations in pH directly affect the concentrations of reactive ions in the medium. At low pH values, the increased concentration of hydrogen ions (H^+) enhances protonation of the reagent or complex sites, which can disrupt coordination and reduce complex stability[24]. Conversely, at higher pH values, the concentration of hydroxide ions (OH^-) rises, promoting the formation of insoluble ferric hydroxides that hinder effective complex formation. At pH = 3.5, a balance between H^+ and OH^- ions are achieved, minimizing any potential side reactions. This moderately acidic environment provides the most favorable condition for strong coordination between the reagent and Fe^{3+} ions, leading to the formation of a stable and well-defined complex, as shown in

Figure 6. Therefore, pH=3.5 is identified as the optimum condition for complete and stable complex formation, as it maintains ionic equilibrium and suppresses unwanted decomposition or precipitation reactions [31,32].

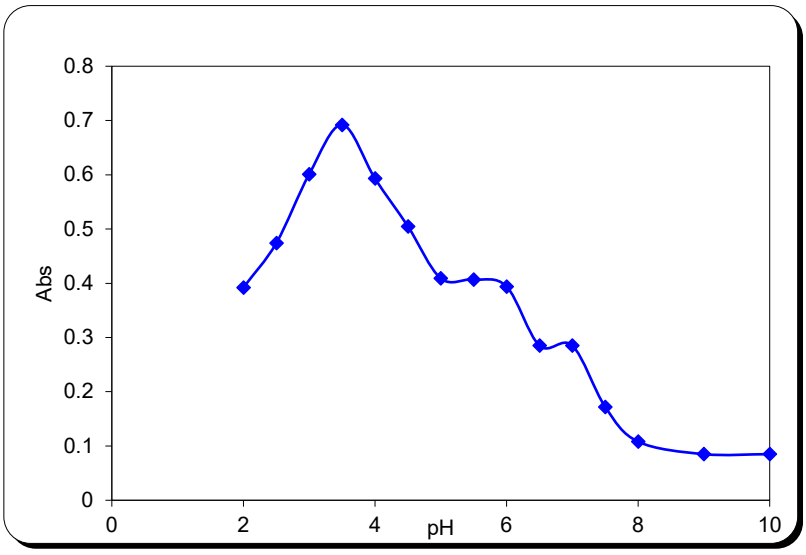

Figure 6. Effect of pH on the Fe complex (Fe=20ppm), (2ml, 1 x 10^{-4} M) of Reagent.

4.2. The temperature and time effect

The complex reaches maximum absorbance after 10 minutes and remains stable for up to 24 hours, indicating high stability, as shown in **Figure 7**. Absorbance is unaffected at temperatures between 10 and 50 °C, while temperatures above 60 °C cause complex dissociation or solvent evaporation, as shown in **Figure 8**. Therefore, the optimal conditions for measurement are 10 minutes and temperatures up to 50°C [33].

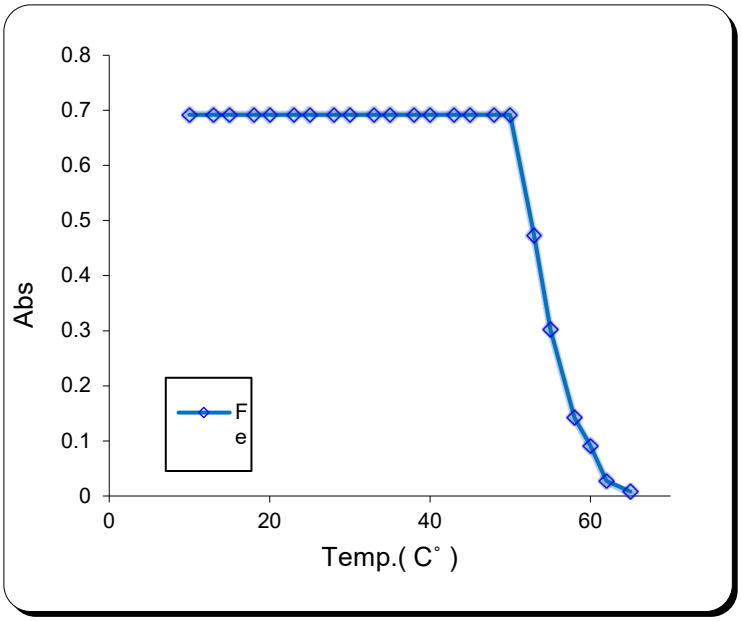

Figure 7. Effect of time on the absorbance of Fe(III) complex (Fe=20ppm), (2ml, 1x10^{-4} M) of Reagent.

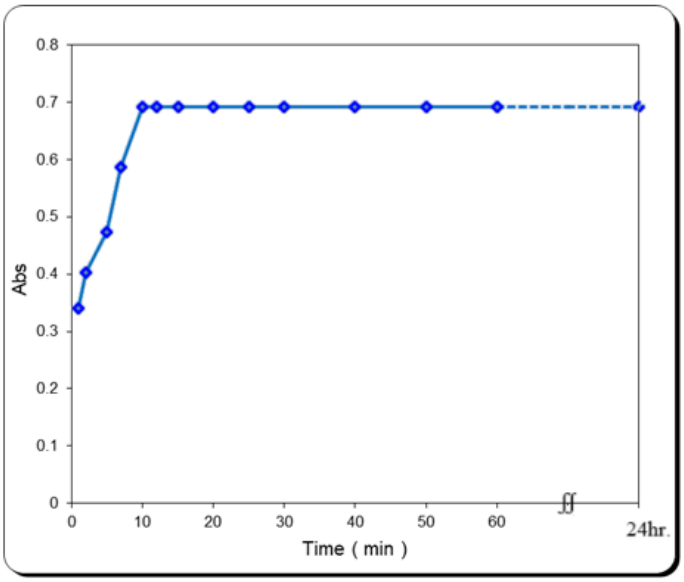

Figure 8. Effect of temperature on the absorbance of Fe(III) complex (Fe=20ppm), (2ml. $1x10^{-4}$ M) of Reagent.

4.3. Complex composition and stability constant

The analysis of the complex composition revealed that Fe (III) ions interact with the reagent in a 1:2 (metal: Reagent) molar ratio, as continuous variations method, as shown in **Figure 9**. and the molar ratio method, as shown in **Figure 10**. The formed complex exhibits high stability at pH 3.5, with a stability constant value (K_{st} = 15 × 10^8 L^2. mol^2) indicating a strong coordination bond that minimizes dissociation in aqueous solution. The dissociation factor (α) was found to be [34],

$$K_{st} = 1/K_{inst} \quad (1)$$

$$K_{inst} = (\alpha C)\,(n\alpha C)^2/C(1-\alpha),\ \alpha = A_m - A_s/A_m \quad (2)$$

Where α =degree of dissociation.

c= total concentration of the complex, n = mole ratio = (2 to Fe(III)).

Am= absorbance of a containing reagent two times excess than the amount of Iron.

As= absorbance of a solution containing a stoichiometric amount [reagent] [Iron].

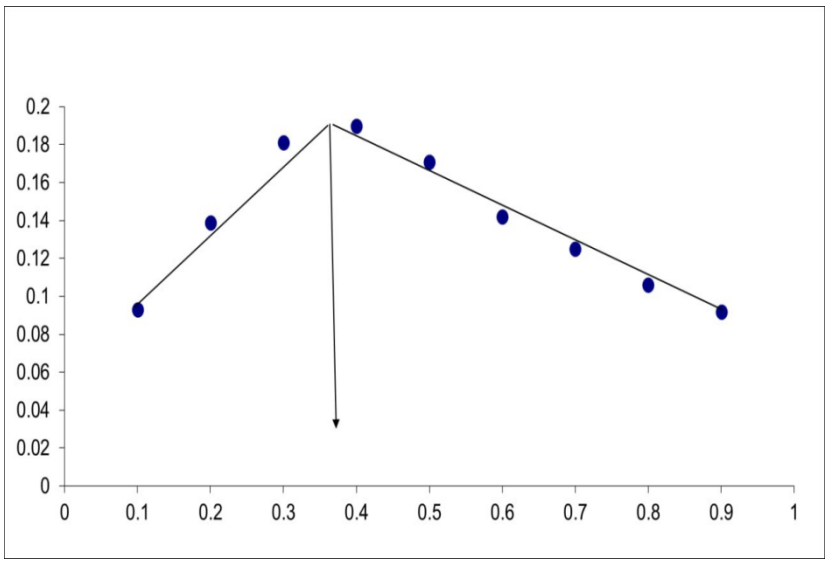

Figure 9. Continuous variation method for Fe (III) complex with (HMNTDABA) at PH=3.5.

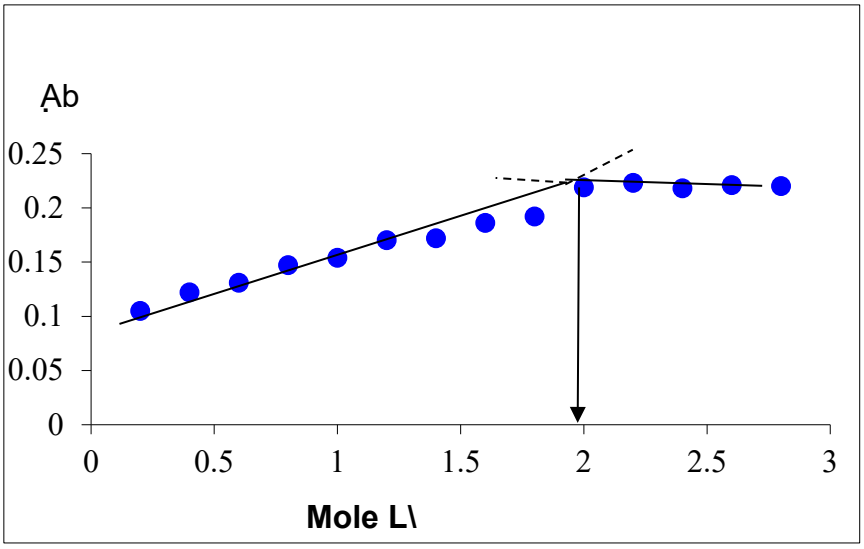

Figure 10. Mole ratio method for Fe (III) complex with (HMNTDABA) at PH=3.5.

4.4. Characteristics of analysis

The calibration curve was established according to the standard experimental procedure, showing an excellent linear relationship between absorbance and Fe (III) concentration over the range of (1-40) ppm, indicating the precision of the analytical method, as shown in **Figure 11**. A summary of the analytical parameters employed in the spectrophotometric determination of Fe(III) using the proposed reagent is presented in the **Table 2**. Furthermore, the Sandell Sensitivity was calculated according to eq.3, reflecting the accuracy and reliability of the spectrophotometric technique [35].

$$\text{Sandell s} = (0.001 \text{ x } 1\text{cm})/\text{slope } (\text{cm}^3/\ \mu\text{g}) \quad (3)$$

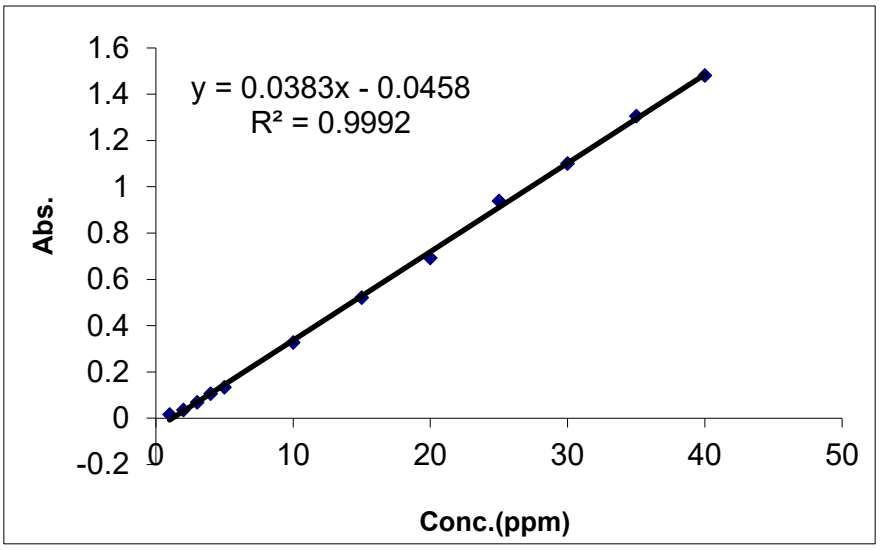

Figure 11. Calibration curve of Fe (III) complex.

Table 2. Analytical data and some analytical parameters for the proposed Fe(III) determination technique.

Analytical Parameter	Fe (III) /ppm
λ_{max}	485 nm

Regression equation	Y=0.0383X – 0.0458
Molar absorptivity ($L.mol^{-}cm^{-}$)	2.139×10^{3}
Sandell Sensitivity	$0.0261L^{-1}$.gm.cm
Corroation coefficient(R)	0.9992
Detection limit(ppm)	0.104
Percent Relative error %	-2.64%
Percent Recovery %	97.36%
Composition of complex (M: L)	1:2
Linear dynamic range(ppm)	1-40
Standerd deviation	0.0012
Relative. Standard. Deviation %	0.17%

4.5. Applications

4.5.1. Biological efficacy

MCF-7 human breast cancer cells were obtained from the Iraqi Center for Cancer and Medical Genetic Research (ICCMGR). Cells were cultured in RPMI-1640 medium supplemented with 10% fetal bovine serum (FBS) and 1% penicillin-streptomycin antibiotic solution, and maintained at 37°C in a humidified atmosphere containing 5% CO_2. Cells were seeded in 96-well plates at a density of 1×10^4 cells/well and allowed to adhere for 24 h before treatment. Cell viability was assessed using the MTT assay after 24 h of exposure to various concentrations of HMNTDABA (3-100 µg/mL). Morphological changes were observed under an inverted phase-contrast microscope.

The biological evaluation of the prepared reagent (HMNTDABA) revealed a significant cytotoxic activity against MCF-7 breast cancer cells in a concentration-dependent manner. Previous studies have demonstrated that oxidative stress biomarkers, such as malondialdehyde (MDA) and polyubiquitin c protein, serve as important indicators in cancer patients [36]. The cell viability decreased progressively with increasing concentration, indicating an effective dose–response relationship as shown in **Table 3**.

Table 3. Cytotoxic effect of (HMNTDABA) on MCF-7 cells after 24 h.

Concentration	Mean	SD	CV (%)
100 µg/ml	39.24646782	1.387572177	0.54457307
75µg/ml	42.87676609	2.081358265	0.89241911
50µg/ml	66.8956044	3.912953538	2.61759392
25µg/ml	86.3422292	3.607687659	3.11495795
10µg/ml	88.85792779	0.882495904	0.78416757
3µg/ml	96.93877551	4.16271653	4.03528643

Microscopic observations confirmed characteristic apoptotic features, including cell rounding, shrinkage, nuclear condensation, and detachment, as shown in **Figure 12**. At higher concentrations, cells transitioned from polygonal morphology to fragmented apoptotic bodies, demonstrating dose-dependent morphological alterations, as shown in **Figure 13**.

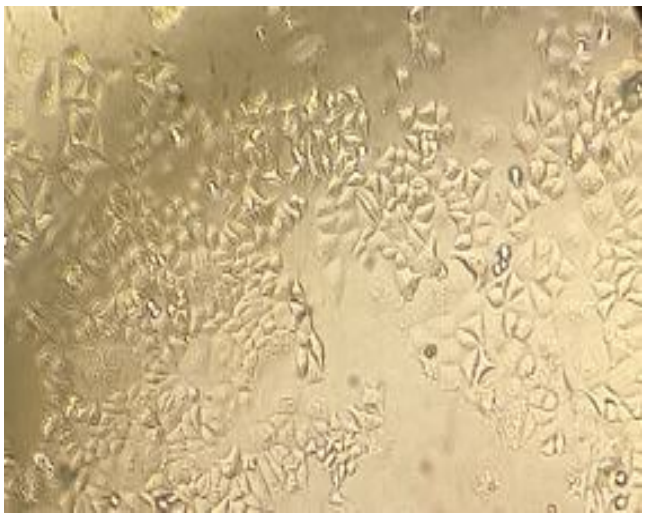

Figure 12. Morphology of untreated MCF-7 control cells after 24 h.

Figure 13. Morphological changes of MCF-7 cells treated with (HMNTDABA) for 24 h.

The compound's structural framework, containing nitro, hydroxyl, and azo functional groups, likely disrupts the cellular redox equilibrium and activates mitochondrial-mediated apoptotic pathways. These findings are consistent with previous studies on heterocyclic azobenzene, thiadiazole, and triazole derivatives [27], which exert comparable cytotoxic effects through LSD1 histone demethylase inhibition [38]. The control MCF-7 cells exhibited intact monolayer morphology with preserved cell-to-cell junctions and no signs of shrinkage or detachment, whereas treated cells displayed marked loss of integrity and reduced density, confirming apoptosis induction by (HMNTDABA) in a dose-dependent fashion as shown in **Figure 14**.

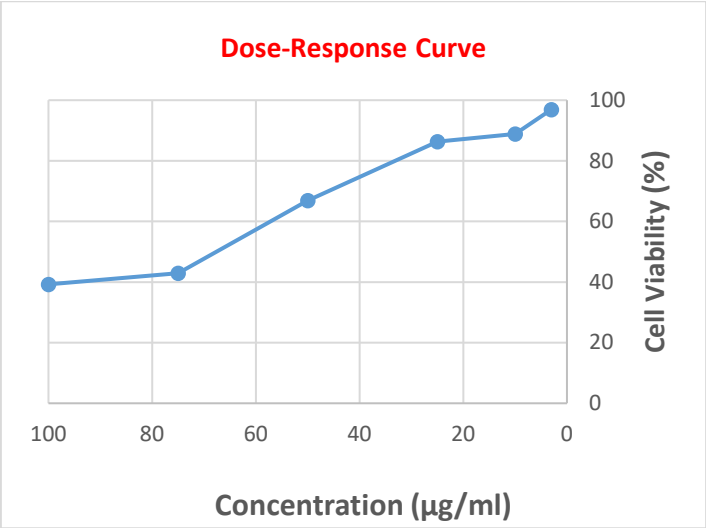

Figure 14. Dose response curve of (HMNTDABA).

4.6. Determination of iron content in anemia medications

The proposed spectrophotometric method employing the reagent (HMNTDABA) was successfully applied for the quantitative determination of iron (III) ion in two commercial pharmaceutical formulations (Ferro Strong) syrup and (Supervit) tablets. Accurate iron determination in anti-anemia medications is particularly important for pediatric patients, where clinical conditions such as abdominal pain and metabolic acidosis can affect drug absorption and therapeutic outcomes [39]. The analytical data summarized in **Table 4** indicate a close agreement between the results obtained by the spectrophotometric method and those obtained by the atomic absorption technique. Each reported value represents the mean of three independent determinations at a 95% confidence level, demonstrating excellent reproducibility and reliability of the proposed method. Furthermore, the obtained concentrations were in good agreement with the labeled contents of the analyzed pharmaceutical products, confirming the method's accuracy and potential applicability as a precise, simple, and rapid alternative for routine pharmaceutical analysis [40].

Table 4. presents the results obtained for the concentrations of iron(III) ion using the reagent (HMNTDABA) by both spectrophotometric and atomic absorption methods.

Method	Tablets	Syrup	The range of the calibration curve
Spectrophotometric	2.482	1.977	(1-40) ppm
Atomic absorption	2.459	1.948	

5. Conclusions

A simple, sensitive, and cost-effective spectrophotometric method was successfully developed for iron(III) determination using the synthesized azo reagent HMNTDABA. The reagent was characterized by FT-IR, UV-Visible spectroscopy, 1H-NMR, XRD, FESEM, and elemental analysis, confirming its proposed structure. Optimal conditions were established at pH 3.5 and 485 nm, where the 1:2 (metal:reagent) complex exhibited maximum stability with a stability constant of 15×10^8 $L^2.mol^{-2}$. The method demonstrated excellent analytical performance with a detection limit of 0.104 ppm, linearity range of 1–40 ppm, and high precision (R.S.D. = 0.17%). Biological evaluation revealed significant dose-dependent cytotoxic activity against MCF-7 breast cancer cells with characteristic apoptotic features. The method was successfully applied for iron(III) determination in Ferro Strong syrup and Supervit tablets, with results comparable to atomic absorption spectroscopy. Therefore, this method provides a rapid and reliable alternative for pharmaceutical iron analysis, while HMNTDABA exhibits in vitro cytotoxicity against MCF-7 breast cancer cells, warranting further mechanistic studies to fully elucidate its therapeutic potential.

Conflict of interest

The authors declare no conflict of interest

References

1. Mohammed, Khadija F., and Hasan A. Hasan. "Synthesis, chemical and biological activity studies of azo-Schiff base ligand and its metal complexes." Chem. Methodol 12 (2022): 905-913.
2. S. Irmuminova, B. Sezgin and T. Tilki, "Novel Heterocyclic Azo Compounds: Synthesis, Characterization and DFT Calculations" in Süleyman Demirel University Faculty of Arts and Science Journal of Science 15(2), (Süleyman Demirel University Faculty, 2020), pp. 319-329,
3. Fattah, Mustafa Subhi, and Shaimaa Mohsen Essa. "Spectrophotometric Determination of Silver Ion in Pharmaceutical Materials Using an Organic Reagent." Advanced Journal of Chemistry, Section A 7.6 (2024): 810-819.
4. Dadi, Murali, and Mohd Yasir. "Spectroscopy and Spectrophotometry: Principles and Applications for Colorimetric." Colorimetry (2022): 81.
5. Vogt, Anne-Cathrine S., et al. "On iron metabolism and its regulation." International journal of molecular sciences 22.9 (2021): 4591.
6. Cain, Timothy J., and Aaron T. Smith. "Ferric iron reductases and their contribution to unicellular ferrous iron uptake." Journal of inorganic biochemistry 218 (2021): 111407.
7. Di Lorenzo, Gianmaria, et al. "Iron alloys and structural steels from XIX century until today: Evolution of mechanical properties and proposal of a rapid identification method." Construction and building materials 302 (2021): 124132.
8. Charlebois, Edouard, and Kostas Pantopoulos. "Nutritional aspects of iron in health and disease." Nutrients 15.11 (2023): 2441.
9. Sahib, H.S., R.K. Mohsin, and S.S. Mutlag, The burden of obesity on children health, its correlation to their age. Revista Latinoamericana de Hipertension, 2021. 15(2): p. 151-157.
10. Mutlag, S.S., The association between iron over load and tanner stage retardation in the females with b-thalassemia major. International Journal of Research in Pharmaceutical Sciences, 2020. 11(1): p. 546-552.
11. Hashim, Z.A. and S.S. Mutlag, Ophthalmologic changes in thalassemia patients. Journal of Pharmaceutical Sciences and Research, 2017. 9(11): p. 2237-2239.
12. Mutlag, S.S., Q.K. Alyasiri, and A.J. Hussein, Causes and clinical management of abdominal pain in pediatric patients. Adolescencia e Saude, 2025. 20(2): p. 15-23.
13. Kontoghiorghes, George J. "The importance and essentiality of natural and synthetic chelators in medicine: increased prospects for the effective treatment of iron overload and iron deficiency." International Journal of Molecular Sciences 25.9 (2024): 4654.
14. Milevskii, N. A., et al. "Separation of Li (I), Co (II), Ni (II), Mn (II), and Fe (III) from hydrochloric acid solution using a menthol-based hydrophobic deep eutectic solvent." Hydrometallurgy 207 (2022): 105777.
15. Ramasekhar, Gunisetty, et al. "Numerical investigation of Casson fluid flow performance of blood containing gold and Fe3O4 nanofluid injected into a stenotic artery." Numerical Heat Transfer, Part A: Applications (2024): 1-17.
16. Michalke, Bernhard. "Review about powerful combinations of advanced and hyphenated sample introduction techniques with inductively coupled plasma-mass spectrometry (ICP-MS) for elucidating trace element species in pathologic conditions on a molecular level." International Journal of Molecular Sciences 23.11 (2022): 6109.
17. Somer, G., O. Sendil, and A. Ünlü. "A new and simple method for the determination of trace Fe (III), Cu (II), Ni (II), Zn (II) and Se (IV) in human hair by differential pulse polarography." Analytical Chemistry Letters 1.5-6 (2011): 328-336.
18. Shahat, Ahmed, Nuha Y. Elamin, and Wesam Abd El-Fattah. "Spectrophotometric and fluorometric methods for the determination of Fe (III) ions in water and pharmaceutical samples." ACS omega 7.1 (2021): 1288-1298.
19. Hadi, Mina Kadhim, and Shaimaa Mohsen Essa. "Spectrophotometric Determination of Silver (I) With 2-Hydroxy-5-(5-(4-Methoxy-3-Nitrophenyl)-1, 3, 4-Thiadiazol-2-yl) Diazenyl) Benzoic Acid (HMNTDABA) as a Nano Organic Reagent." Journal of Nanostructures 15.3 (2025): 916-927.
20. Ali, Luay, and Shaimaa Adnan. "Synthesis and characterization of new diazo derivatives, and study of their biological activity." IJDDT 12.1 (2022): 232-236.
21. Kholboyeva, M. B., et al. "Determination of Fe (III) ion with a novel, highly efficient immobilized nitrosa R-salt in a polymer matrix." Chemical Review and Letters 8.3 (2025): 448-459.
22. Al-Hussainawy, Mohammed Kassim, and Layth S. Jasim Al-Hayder. "Drug carriers in the delivery and release of hydroxychloroquine by biopolymer." Chemical Papers 78.9 (2024): 5255-5266.
23. A. Mohsin, M. Radhi and W. Hoidy, "Study the gold compound (aucu) in kel using cyclic voltammetry by nano sensor" in Research Journal of Pharmacy and Technology 14(6). (A and V Publication, 2021), pp. 3004-3008.
24. Al-Hayder, Layth S. Jasim. "Drug carriers in the delivery and release of hydroxychloroquine by biopolymer." (2023).
25. Mayeen, Anshida, et al. "Morphological characterization of nanomaterials." Characterization of nanomaterials. Woodhead Publishing, 2018. 335-364.

26. Belowar, Sanjay. "Synthesis and biological study of newly synthesized AZO appended thiadiazolin heterocycles." (2022).
27. Selivanova, Galina, et al. "Azo dyes containing 1, 3, 4-thiadiazole fragment: synthesis and properties." New Journal of Chemistry 46.4 (2022): 1929-1942.
28. K. AL-Adilee, L. Al-Hayder and S. Essa, " Synthesis and Antioxidant Activity Evaluation of New Organic Reagent 2-[2-(5-Nitro thiazolyl) azo]-4, 6-dimethoxy benzoic acid (NTADMBA)" In: Journal of Physics: Conference Series 1664(1), (Conferences and Proceedings, 2020), pp. 012059.
29. V. Kothavale, A. Sharma, R. Dhavale, V. Chavan. S. Shingte, O. Selyshchev, and et al "Carboxyl and thiol-functionalized magnetic nanoadsorbents for efficient and simultaneous removal of Pb (II), Cd (II), and Ni (II) heavy metal ions from aqueous solutions: Studies of adsorption, kinetics, and isotherms" in Journal of Physics and Chemistry of Solids 172. (Elsevier Ltd. 2023), pp. 111089.
30. H. Karapinar, F. Kilicel, F. Ozel, and A. Sarilmaz, "Fast and effective removal of Pb (II), Cu (II) and Ni (II) ions from aqueous solutions with TiO2 nanofibers: Synthesis, adsorption-desorption process and kinetic studies" in International Journal of Environmental Analytical Chemistry 103(16), (Taylor and Francis Ltd, 2023), pp. 4731-4751.
31. Abdullah, Asmaa M., Mohammed Mujbel Hasson, and Mohammed Z. Thani. "Synthesis, thermal analysis, spectroscopy and magnetic properties of some transition metals complexes derived from new azo compound." Materials Today: Proceedings 20 (2020): 595-598.
32. A. Hassan, and A. Amin, "El-Maghrabey M, et al. Sustainable non-plasticized polymer inclusion membrane containing an immobilizing optode ligand for in situ ultra-sensitive colorimetric measurement and pre-concentration of beryllium ions in environmental and biological matrices" in Journal of Photochemistry and Photobiology A: Chemistry 452, (Elsevier B.V, 2024), pp. 115624.
33. Abdelazim, Ahmed H., and Sherif Ramzy. "Spectrophotometric quantitative analysis of remdesivir using acid dye reagent selected by computational calculations." Spectrochimica Acta Part A: Molecular and Biomolecular Spectroscopy 276 (2022): 121188.
34. Alsfouk, B.A., et al., Integrated computational and biological evaluations of newly synthesized thiadiazole-based VEGFR-2 inhibitors with targeted anti-breast cancer activity. Naunyn-Schmiedeberg's Archives of Pharmacology, 2025: p. 1-23.
35. Alqahtani, N.F., et al., Molecular docking and in vivo/in vitro studies of a novel thiadiazole Schiff base as a hepatoprotective drug against angiogenesis induced by breast cancer. RSC advances, 2024. 14(52): p. 39027-39039.
36. Alsehli, M., et al., Design and synthesis of benzene homologues tethered with 1, 2, 4-triazole and 1, 3, 4-thiadiazole motifs revealing dual MCF-7/HepG2 cytotoxic activity with prominent selectivity via histone demethylase LSD1 inhibitory effect. International Journal of Molecular Sciences, 2022. 23(15): p. 8796.
37. Sahib, H.S., R.K. Mohsin, and S.S. Mutlag, Assessment the concentration of malondialdehyde MDA and polyubiquitin c protein in patients with breast and gastric cancer. Revista Latinoamericana de Hipertension, 2021. 15(3): p. 232-238.
38. Sahib, H.S., R.K. Mohsin, and S.S. Mutlag, Analyzing the issue of overweight and children health. Revista Latinoamericana de Hipertension, 2021. 15(3): p. 260-266.
39. Mutlag, S.S., Metabolic acidosis impairs clearance of upec-uti. Research Journal of Pharmacy and Technology, 2020. 13(1): p. 330-334.
40. G.W. Ewing, "Instrumental Methods of Chemical Analysis", 4th Edition, McGraw-Hill, NeW York, P.515, (1975).